Received July 6, 2021, accepted July 16, 2021, date of publication July 20, 2021, date of current version August 11, 2021.

Digital Object Identifier 10.1109/ACCESS.2021.3098953

Viscoelastic Evaluation of Composite Materials by Non-Contact Air Coupled Ultrasonic Transmission Method

JUNJIE CHANG[1,2], CONGCONG WANG[1], WENCHAO LI[1], YUAN TANG[2], AND ZHIHENG CHEN[1]
[1]Key Laboratory of Nondestructive Testing, Ministry of Education, Nanchang Hangkong University, Nanchang 330063, China
[2]College of Optoelectronic Engineering, Chongqing University of Posts and Telecommunications, Chongqing 400065, China

Corresponding author: Congcong Wang (wccwcwcc@163.com)

This work was supported by the National Natural Science Foundation of China under Grant 11464030.

ABSTRACT The viscoelasticity of composite materials is one of the important mechanical properties to characterize the intrinsic damping mechanism, which is a crucial evaluation index for the safety performance of materials. In this paper, an approach to viscoelastic evaluation is proposed by the non-contact air-coupled ultrasonic transmission method (NACUTM). The theory of viscoelasticity evaluation is presented, and a batch of carbon fiber composite materials with different pores were evaluated. The porosity of the carbon fiber composite material can affect the ultrasonic attenuation coefficient and viscoelasticity of the material, and it was found and compared with the C-scan test result. The results were consistent with the expected value, which verified the feasibility and accuracy of NACUTM in material viscoelastic evaluation, and provided a new method for dynamic mechanical property evaluation and safety evaluation of the composite materials.

INDEX TERMS Composite material, physical properties, non-contact air-coupled ultrasonic, transmission method.

I. INTRODUCTION

Composite materials are widely used in aerospace, automobile, ship, high-speed railway and other fields because of their excellent characteristics such as high specific strength, high specific stiffness, fatigue resistance, strong vibration damping capacity and high-temperature resistance [1], [2]. However, composite materials are applied in complex environment, which can be subject to adverse factors such as vibration and impact. Moreover, these adverse factors act continuously, which leads to structural fatigue and damage of composite materials and shorten the service life of composite materials [3]–[7]. Therefore, it is extremely urgent to study the safety performance of composite materials. Traditional ultrasonic testing requires couplers which make the composites damp and polluted, and even enter into the material along with the defect. The couplers can result in the change of mechanical properties of the materials [8]–[11].

The internal damping mechanism of composite materials is a significant evaluation index for the safety performance of materials, and the viscoelasticity of composite materials is an important mechanical property to represent the internal damping mechanism. In order to ensure the safety of composite materials, it is necessary to evaluate the viscoelasticity of composite materials [12]–[16]. At present, the evaluation methods of viscoelasticity of composite materials mainly include dynamic mechanical analysis (DMA) and the method of ultrasonic [17]–[20]. However, for in-service components and special structural composite materials (such as carbon fiber reinforced plastic (CFRP)), the above methods are powerless, and the coupling agent and water also have a great impact on the mechanical properties of composite materials.

The air-coupled ultrasonic detection technology has the characteristics of non-contact, non-infiltration, and non-damage, which is especially suitable for the detection of composite materials [21]–[23]. In this paper, a viscoelasticity evaluation method of composite materials is studied based on air-coupled ultrasound. The theories of viscoelasticity and ultrasonic composite evaluation method is analyzed, and the comparison between the C-scan test result and the NACUTM is investigated. The feasibility and accuracy of this method are verified. In this study, real non-contact non-destructive

The associate editor coordinating the review of this manuscript and approving it for publication was Giovanni Angiulli.

testing technology can be realized, and it can carry out non-destructive testing for some dangerous goods that cannot be directly contacted. These dangerous goods can be sulfuric acid, explosives, etc. Therefore, in the future non-contact non-destructive testing technology of the physical properties of materials, this research has important reference value.

II. DETECTION PRINCIPLE

A. VISCOELASTIC EVALUATION METHOD

The static and dynamic viscoelasticity of materials is evaluated from different aspects. The composite material is subjected to the dynamic force. The dynamic mechanical properties can reflect the material performance better than the static mechanical properties in the actual working conditions. Sinusoidal stress is the most commonly used alternating stress in dynamic mechanical experiments. Taking the tensile stress as an example, the strain is as follows,

$$\sigma_\tau(t) = \sigma_{\tau 0} \sin \omega t \tag{1}$$

where $\sigma_{\tau 0}$ is the stress amplitude, ω is the angular frequency (rad).

The strain response of materials by sinusoidal alternating stress varies with their properties. For an ideal elastomer, the strain response of stress is instantaneous. The strain response is a sine function in the same phase with the stress, and the expression of strain is shown as,

$$\varepsilon(t) = \varepsilon_0 \sin \omega t \tag{2}$$

where ε_0 is the strain amplitude.

For an ideal viscous body, the strain lags behind the stress by 90°. For viscoelastic materials, the strain lags one phase angle of stress $\delta(0° < \delta < 90°)$. When $\varepsilon(t) = \varepsilon_0 \sin \omega t$, then $\sigma(t) = \sigma_0 \sin(\omega t + \delta)$, the stress expression is shown as,

$$\sigma(t) = \sigma_0 \sin \omega t \cos \delta + \sigma_0 \cos \omega t \sin \delta. \tag{3}$$

It can be seen from the Eq. (3) that the stress consists of two parts: one is the stress in the same phase with the strain, that is, $\sigma_0 \sin \omega t \cos \delta$, which is the main force of elastic deformation; another is the stress with a 90° phase difference from the strain, namely $\sigma_0 \cos \omega t \sin \delta$. Since the deformation corresponding to this stress is viscous deformation, it will be consumed to overcome the frictional resistance. If E' is defined as the ratio of the stress and strain amplitudes of the same phase, E'' is the ratio of the stress and strain amplitudes differing by 90°, then,

$$E' = \frac{\sigma_0 \cos \delta}{\varepsilon_0} = \frac{\sigma_0}{\varepsilon_0} \cos \delta \tag{4}$$

and

$$E'' = \frac{\sigma_0 \sin \delta}{\varepsilon_0} = \frac{\sigma_0}{\varepsilon_0} \sin \delta. \tag{5}$$

Incorporating Eq. (4) and Eq. (5) into Eq. (3), the expression is as follows,

$$\sigma(t) = E'\varepsilon_0 \sin \omega t + E''\varepsilon_0 \cos \omega t. \tag{6}$$

where E' is real modulus or storage modulus, and E'' is virtual modulus or loss modulus.

Therefore, the formula (6) includes two parts, and the expression of the modulus conforms to the mathematical form of the complex number, which is called the complex modulus (E^*), the expression is shown as,

$$E^* = E' + iE'' \tag{7}$$

The calculation formula of the tangent value of the loss tangent is shown in Eq. (8),

$$\tan \delta = \frac{E''}{E'}. \tag{8}$$

B. DETECTION METHODS AND PROCEDURES

The viscoelasticity of materials is evaluated by using the NACUTM, and the evaluation steps are as follows.

1) ANALYZE ATTENUATION COEFFICIENT OF ULTRASONIC WAVE IN AIR

A schematic diagram of calculating the attenuation coefficient of ultrasonic waves in air is shown in Fig. 1.

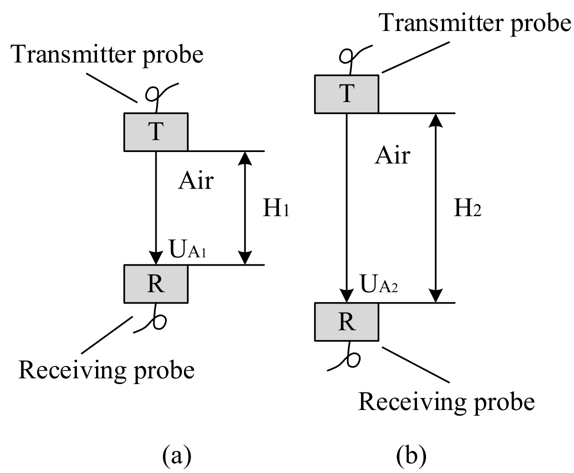

FIGURE 1. A schematic diagram of calculating the attenuation coefficient of ultrasonic waves in air. (a) The distance between the two probes is H1. (b) The distance is between the two probes are H2.

The viscoelastic properties of materials are evaluated using the NACUTM, and the attenuation coefficient $a_1(f)$ of ultrasonic waves in air can be obtained as the following steps. Firstly, adjust the distance between the transmitting and receiving probes to be H_1, and the first received waveform is denoted as U_{A1}. Then adjust the distance between the transmitting and receiving probes to be H_2, and the first received waveform is denoted as U_{A2}. Lastly, the spectrum of the received waveform U_{A1} and U_{A2} were analyzed, and the obtained amplitude spectrum was denoted as $A_1(f)$ and $A_2(f)$. The attenuation coefficient $a_1(f)$ of ultrasonic wave in air can be calculated by Eq. (9),

$$a_1(f) = \frac{20}{H_2 - H_1} lg(\frac{A_1(f)}{A_2(f)}). \tag{9}$$

2) SOUND PRESSURE REFLECTANCE AT INTERFACE BETWEEN EXPERIMENTAL MATERIAL AND AIR

As shown in Fig. 2, the distance between the transmitting and receiving probes is adjusted to d, and the incident wave received by the probe is denoted as U_0, as shown in Fig. 2(a). Then, the ultrasonic detection is used by echo method. A single probe is used to adjust the distance between the transmitting probe and the upper surface of the material to $d/2$. The interface reflected wave received by the probe is denoted as U_1 as shown in Fig. 2(b). Finally, the spectrum of the signal U_0 and U_1 is analyzed, and the obtained amplitude spectrum is denoted as $U_0(f)$ and $U_1(f)$. According to Eq. (10), the reflectance of the sound pressure at the interface between material and air can be obtained as,

$$r(f) = \frac{U_1(f)}{U_0(f)} \tag{10}$$

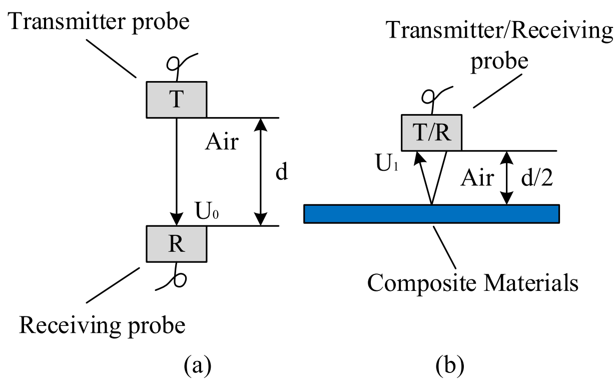

FIGURE 2. A schematic diagram of calculating the interface sound pressure reflectivity. (a) Direct receiving the ultrasonic wave. (b) Receiving the reflection wave.

3) ATTENUATION COEFFICIENT OF ULTRASONIC WAVE IN MATERIAL

As shown in Fig. 3, firstly, adjust the distance between the transmitting and receiving probes to be d, and record the received signal as U_A as shown in Fig. 3(a), then put the tested material between the transmitting and receiving probes, and keep the material perpendicular to the transmitting probe. The ultrasonic wave can enter the material vertically. The distance between the transmitting and receiving probes is D, and the received signal is denoted as U_B as shown in Fig. 3(b). The received signal U_A and U_B was used for spectral analysis, and the amplitude spectrum was denoted as $A(f)$ and $B(f)$, respectively. According to Eq. (11), the attenuation coefficient of ultrasonic wave in the material can be obtained,

$$a(f) = a_1(f) + \frac{20}{h} lg[\frac{A(f)}{B(f)}(1 - r^2(f))] \tag{11}$$

where, h is the thickness of the tested material.

4) PHASE VELOCITY

According to the sum of the amplitude spectrum $A(f)$ and $B(f)$, the phase angle of the signal U_A and U_B can be

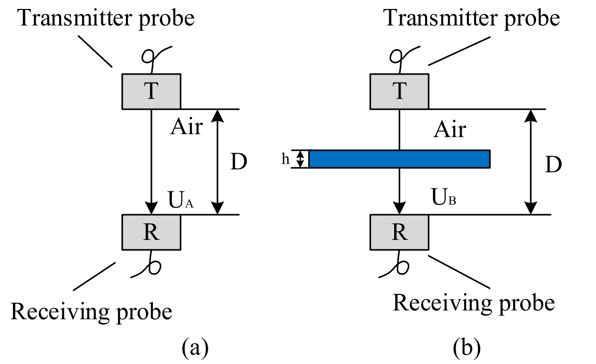

FIGURE 3. Schematic diagram of experimental materials placed/not placed between two probes. (a) No material is placed between the two probes to receive ultrasonic wave. (b) Put carbon fiber between the two probes to receive ultrasonic wave.

calculated by Eq. (12), respectively,

$$\theta_A(f) = tan^{-1}\frac{Im[A(f)]}{Re[A(f)]}, \quad \theta_B(f) = tan^{-1}\frac{Im[B(f)]}{Re[B(f)]} \tag{12}$$

where $Im[A(f)]$ is the imaginary part of the spectrum of signal U_A, $Re[A(f)]$ is the real part of the signal spectrum U_A, $Im[B(f)]$ is the imaginary part of the spectrum of signal U_B, $Re[B(f)]$ is the real part of the spectrum of signal U_B. According to the Eq. (12) and the wave number $\beta = 2\pi f/C_P$, the phase velocity can be obtained by Eq. (13),

$$\frac{1}{C_p(f)} = \frac{\theta_B(f) - \theta_A(f)}{\omega h} + \frac{1}{C_a} \tag{13}$$

where, ω is angular velocity ($\omega = 2\pi f$), h is the thickness of the material, C_a is the sound velocity in air.

In order to obtain the absolute phase angle of the signal, the Fourier transform is applied to the signal. The signal between $t = 0$ and the time that the signal begins to be received needs to be zeroized, and the Fourier transform is applied to the whole signal. Due to the complexity of this process, in order to simplify the solution of the absolute phase angle, the following method is used to obtain the absolute phase angle of the ultrasonic signal.

When the spectrum of the signals U_A and U_B is analyzed, the time t_A and t_B corresponds to signals U_A and U_B, respectively. The time difference T is

$$T = t_B - t_A. \tag{14}$$

Then the phase velocity C_P can be obtained by using the real and imaginary parts of the frequency spectrum of the signal,

$$\frac{1}{C_p(f)} = \frac{\theta_B(f) - \theta_A(f)}{\omega h} + \frac{1}{C_a} + \frac{T}{h} \tag{15}$$

where f is the frequency, ω is the angular frequency, C_a is the wave velocity in the air.

According to the complex elasticity theory, the energy storage modulus E', energy dissipation modulus E'' and $\alpha Vp/\omega \ll 1$, the tangent of loss tangent of the P-wave

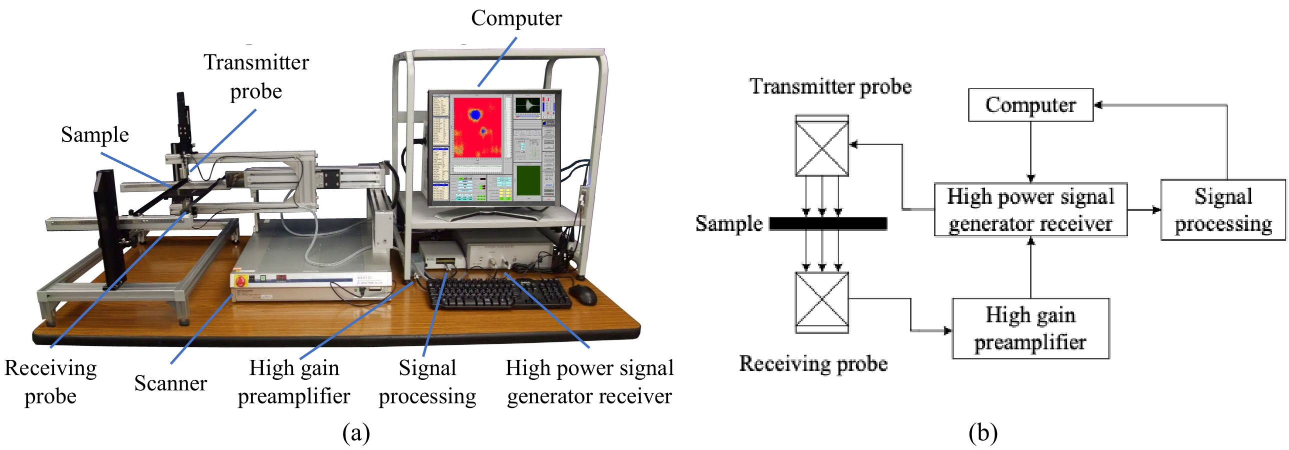

FIGURE 4. Schematic diagram of air coupled ultrasonic testing system. (a) Ultrasonic transmitter/receiver and clamp for actual measurement. (b) Measurement system of ultrasonic air-coupled transmission method experiment.

ultrasonic wave can be deduced from Eq. (16).

$$\begin{cases} E' = \rho C_p^2 \\ E'' = \dfrac{2\alpha\rho C_p^3}{\omega} = \dfrac{2\alpha C_p}{\omega} E' \\ tan\delta = \dfrac{E''}{E'} = \dfrac{2\alpha C_p}{\omega} \end{cases} \tag{16}$$

By using Eq. (16), the viscoelasticity of the material can be evaluated.

III. TESTING SYSTEMS AND VISCOELASTICITY EVALUATION OF CARBON FIBER COMPOSITE MATERIALS

A. EXPERIMENTAL SYSTEMS AND MATERIALS

The schematic diagram of air-coupling ultrasonic testing systems is shown in Fig. 4, including computer (NUAT system control based on LabVIEW software), NI data acquisition unit (PXT-1033), transceiver of high-power ultrasonic signal (Japan Probe Co., ltd. JPR-600C), preamplifier (gain is 60 dB), air-coupling plate probe (frequency of 0.8 MHz, the size of the piezoelectric wafer to 14mm × 20mm).

In order to investigate the influence of different porosity on the material viscoelasticity, a number of different porosities of 15mm carbon fiber composite material is made. The distance is 42.5mm between the probe and the surface of the sample. And the distance is 100mm between the transmitter probe and receiving probe. The selection of four different porosity of carbon fiber composites are A, B, C, D four areas, respectively. The photograph of carbon fiber composites is as shown in Fig. 5(a) for C scan, and the area of the four holes are as shown in Fig. 5(b). The red area in C-scan results is the area with higher ultrasonic penetration ability, while the blue area is the area with lower ultrasonic penetration ability [24].

B. EXPERIMENT AND DATA ANALYSIS

1) FOUR DIFFERENT AREAS OF STOMA CARBON FIBER COMPOSITE MATERIALS

When the spacing between the two probes is 65mm and 90mm, respectively, the ultrasonic wave received by the probe is recorded as U_{A1} and U_{A2} respectively, and its waveform is shown in Fig. 6(a) and in Fig. 6(b).

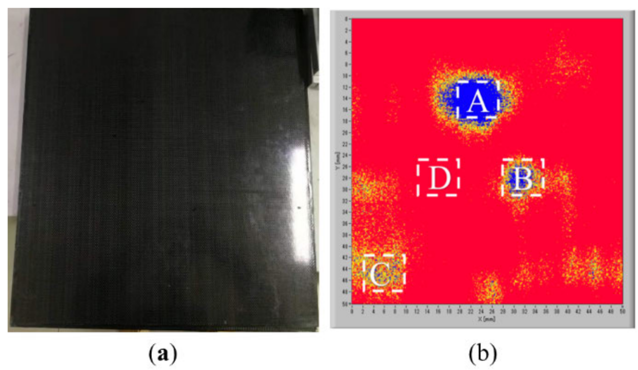

FIGURE 5. Carbon fiber composite material diagrams. (a) Carbon fiber material. (b) The results of C-scan.

Spectrum analysis was carried out in the area of the first enveloping point. The amplitude spectrum of waveform U_{A1} and U_{A2} were obtained respectively. According to the calculation formula of attenuation coefficient of ultrasonic wave in air, the attenuation coefficient results were obtained, as shown in Fig. 6(c). When the frequency of ultrasonic wave is 0.8MHz, the attenuation coefficient of ultrasonic wave in air is 0.175db/mm. It is found that the higher the frequency of ultrasonic demonstrates the higher the attenuation of ultrasonic in the air.

When the distance between the two probes is adjusted to 100mm, carbon fiber material and no material are placed between the two probes, and the four different areas of A, B, C, and D are air-coupled. For the area A, the waveform without material is recorded as A_a, and the waveform with carbon fiber material is recorded as A_b. The waveform is shown in Fig. 7.

Air coupling was carried out at four different positions A, B, C and D respectively to obtain the waveforms. Spectrum analysis of the waveforms was conducted to obtain the

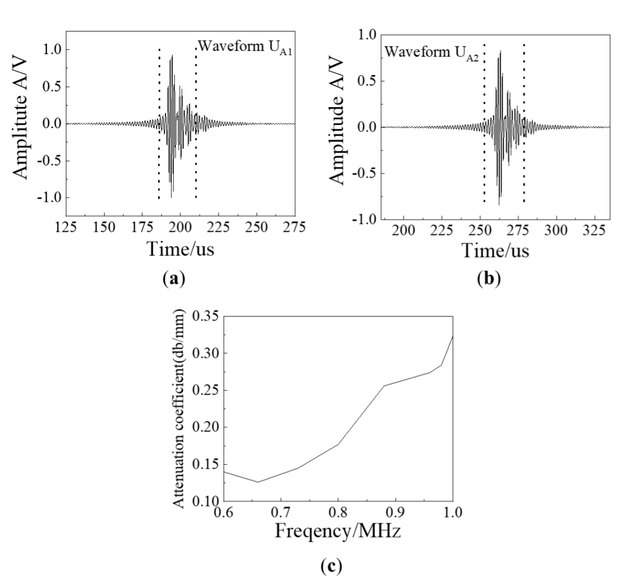

FIGURE 6. The received waveform and air attenuation coefficient at different distances. (a) The received waveform at the distance of 65mm. (b) The received waveform at the distance of 90mm. (c) The relation between attenuation coefficient and frequency in air.

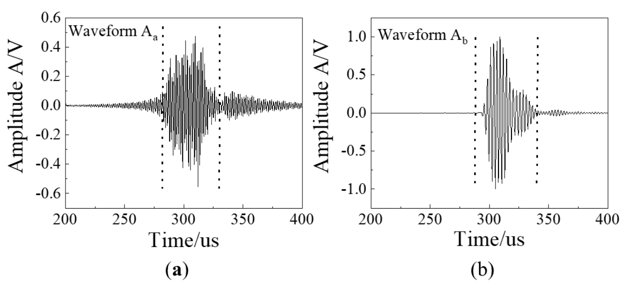

FIGURE 7. The waveform of the area A. (a) No material is placed between the two probes. (b) The waveform recorded by two probes performing air-coupled ultrasound on the area A.

amplitude spectrum of the waveforms. Then, according to the formula for calculating the attenuation coefficient and loss tangent of ultrasonic wave in the material, the relationship between the attenuation coefficient and frequency at four different positions and the tangent value of the loss tangent and frequency is obtained, as shown in Fig. 8.

2) ANALYSIS OF VISCOELASTIC EVALUATION RESULTS OF COMPOSITE MATERIALS

The theoretical background could be enriched with recent work of sound transmission through multilayered structures with viscoelastic layers [25], [26]. The viscoelasticity of carbon fiber composites with different pores was evaluated by the air-coupling penetration method, and the evaluation results of viscoelasticity of carbon fiber composites with different pores were obtained. After the above results are rearranged, the tangents of loss tangent $\tan\delta$ of carbon fiber composites with different porosity and different frequencies are obtained. As shown in Fig. 8, the results show that the

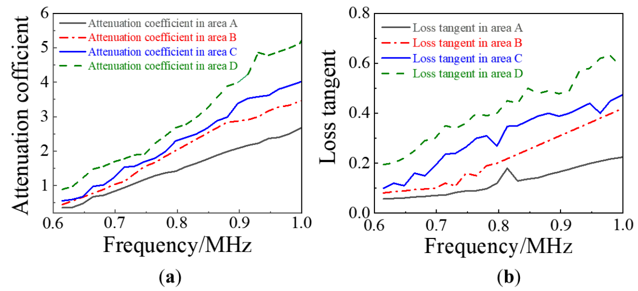

FIGURE 8. The attenuation coefficient and tangent value of the loss tangent of the ultrasonic wave in the material. (a) Attenuation coefficient of ultrasonic wave at four different pore locations. (b) The loss tangent of the carbon fiber at four different pore locations.

tangents of loss tangent $\tan\delta$ of carbon fiber composites decrease with the increase of the ultrasonic frequency. The porosity of the material has a certain effect on the attenuation coefficient of the material. The attenuation coefficient of ultrasonic wave propagation in large pore area is smaller than that in the small pore area. The tangent of loss tangent in the area with high pore density is less than that in the area with low pore density. As shown in Fig. 5(b) and Fig. 8(a), the attenuation of ultrasonic wave in different areas of the material can also be well correlated with the results of C-scan.

IV. CONCLUSION

In this paper, the method of evaluating the viscoelasticity of carbon fiber composites by air-coupled ultrasonic penetrating method is proposed. The ultrasonic attenuation coefficient and viscoelasticity of carbon fiber composite materials were measured successfully. It is concluded that the porosity of carbon fiber composite material can affect the ultrasonic attenuation coefficient and the viscoelasticity of the material, and the consistency between the porosity distribution and the C-scan test results is proved by comparing with the C-scan results. It provides a new evaluation method for some materials that cannot be evaluated by the contact method. The experiment verified the feasibility of the air-coupled ultrasonic method in the viscoelastic evaluation of composite materials.

REFERENCES

[1] S. Y. Du, "Advanced composite materials and aerospace," *Acta Mater. Compos. Sinica*, vol. 12, no. 1, pp. 1–14, 2006.
[2] J. Chang, K. Yang, and G. Li, "Application of air-coupled ultrasonic technology in Li-on battery defect detection," *Battery Bimonthly*, vol. 47, no. 5, pp. 315–317, 2017.
[3] E. Pošković, F. Franchini, M. A. Grande, L. Ferraris, and R. Bidulský, "Innovative soft magnetic composite materials: Evaluation of magnetic and mechanical properties," *Open Eng.*, vol. 8, no. 1, pp. 368–372, Nov. 2018.
[4] G. Rusu and E. Rusu, "Anionic nylon 6/zinc composite materials: Evaluation of thermal and mechanical behavior," *Int. J. Polym. Anal. Characterization*, vol. 15, no. 8, pp. 509–523, Nov. 2010.
[5] W. A. Grandia and C. M. Fortunko, "NDE applications of air-coupled ultrasonic transducers," in *Proc. IEEE Ultrason. Symp.*, vol. 1, Nov. 1995, pp. 697–709.
[6] W. Gao, "Discussion on the influence of scanning direction of composite material on the results of water-jet ultrasonic C-scan," *Nondestruct. Test.*, vol. 44, no. 2, pp. 13–16, 2020.

[7] G. Li, J. Wang, A. Ni, G. Zhang, and W. Guo, "Ultrasonic attenuation model of porosity of CFRP/epoxy composites of different thickness," *J. Compos. Mater.*, vol. 31, no. 4, pp. 877–885, 2020.
[8] S. Gunasekaran and M. M. Ak, "Dynamic oscillatory shear testing of foods—Selected applications," *Trends Food Sci. Technol.*, vol. 11, no. 3, pp. 115–127, Mar. 2000.
[9] X. Zeng, C.-L. Yang, X.-J. Zhou, and G.-Y. Teng, "Ultrasonic resin-rich detection of carbon fiber composites with Small porosity," *Opt. Precis. Eng.*, vol. 26, no. 11, pp. 2732–2743, 2012.
[10] W. Zhu, Y. Xiang, C.-J. Liu, M. Deng, and F.-Z. Xuan, "A feasibility study on fatigue damage evaluation using nonlinear Lamb waves with group-velocity mismatching," *Ultrasonics*, vol. 90, pp. 18–22, Nov. 2018.
[11] S. Gholizadeh, "A review of non-destructive testing methods of composite materials," *Proc. Struct. Integr.*, vol. 1, pp. 50–57, Jan. 2016.
[12] R. A. Schapery, "Stress analysis of viscoelastic composite materials," *J. Compos. Mater.*, vol. 1, no. 3, pp. 228–267, Jul. 1967.
[13] B. Yates, B. A. McCalla, L. N. Phillips, D. M. Kingston-Lee, and K. F. Rogers, "The thermal expansion of carbon fiber-reinforced plastics. Part 5: The influence of matrix curing characteristics," *J. Mater. Sci.*, vol. 14, no. 5, pp. 1207–1217, 1979.
[14] J. Hodges, B. Yates, M. I. Darby, G. H. Wostenholm, J. F. Clemmet, and T. F. Keates, "Residual stresses and the optimum cure cycle for an epoxy resin," *J. Mater. Sci.*, vol. 24, no. 6, pp. 1984–1990, Jun. 1989.
[15] D. Jalocha, A. Constantinescu, and R. Nevière, "Prestrained biaxial DMA investigation of viscoelastic nonlinearities in highly filled elastomers," *Polym. Test.*, vol. 42, pp. 37–44, Apr. 2015.
[16] J. Chang, C. Lu, and Y. Ogura, "Principle and application research of non-contact air-coupled ultrasonic detection," *Nondestruct. Test.*, vol. 31, no. 4, pp. 6–11, 2013.
[17] X. J. Gao and Z. Zhang, "Research of the relationship between pore morphology and ultrasonic attenuation coefficient in CFRP," *J. Mater. Eng.*, vol. 2, no. 7, pp. 59–63, 2012.
[18] X. Zhang, J. Chen, L. Li, and X. M. Li, "Effects on ultrasonic scattering attenuation coefficient of morphological characteristics of voids in composite materials," *China Mech. Eng.*, vol. 21, no. 14, pp. 1735–1741, 2010.
[19] R. Kažys, A. Demčenko, E. Žukauskas, and L. Mažeika, "Air-coupled ultrasonic investigation of multi-layered composite materials," *Ultrasonics*, vol. 44, pp. e819–e822, Dec. 2006.
[20] A. Y. Aköz, F. Kadıoğlu, and G. Tekin, "Quasi-static and dynamic analysis of viscoelastic plates," *Mech. Time-Dependent Mater.*, vol. 19, no. 4, pp. 483–503, Nov. 2015.
[21] M. Imiela, R. Anyszka, D. M. Bieliński, Z. Pędzich, M. Zarzecka-Napierała, and M. Szumera, "Effect of carbon fibers on thermal properties and mechanical strength of ceramizable composites based on silicone rubber," *J. Thermal Anal. Calorimetry*, vol. 124, no. 1, pp. 197–203, Apr. 2016.
[22] E. van Ruymbeke, R. Keunings, and C. Bailly, "Determination of the molecular weight distribution of entangled linear polymers from linear viscoelasticity data," *J. Non-Newtonian Fluid Mech.*, vol. 105, nos. 2–3, pp. 153–175, Aug. 2002.
[23] J. Chang, C. Lin, and D. Sun, "Evaluation of rubber friction materials viscoelasticity by ultrasonic wave method," *Lubrication Eng.*, vol. 31, no. 11, pp. 55–58, 2007.
[24] M. Sántos, J. Santos, P. Reis, and A. Amaro, "Ultrasonic C-scan techniques for the evaluation of impact damage in CFRP," *Mater. Test.*, vol. 63, no. 2, pp. 131–137, Feb. 2021.
[25] S. Valvano, A. Alaimo, and C. Orlando, "Analytical analysis of sound transmission in passive damped multilayered shells," *Compos. Struct.*, vol. 253, Dec. 2020, Art. no. 112742.
[26] S. Valvano, A. Alaimo, and C. Orlando, "Sound transmission analysis of viscoelastic composite multilayered shells structures," *Aerospace*, vol. 6, no. 6, p. 69, Jun. 2019.

JUNJIE CHANG was born in Dalian, China, in 1964. She received the Ph.D. degree from Kyoto University of Technology and Fiber, in 2005. She is currently a Professor with Chongqing University of Posts and Telecommunications. Her research interest includes the development of acoustic detection technology and equipment.

CONGCONG WANG was born in Henan, China, in 1998. He received the B.Sc. degree from Nanchang Hangkong University, in 2020, where he is currently pursuing the M.E. degree. His research interests include acoustic nondestructive testing and signal processing for the anisotropic and heterogeneous materials.

WENCHAO LI was born in Jiangxi, China, in 1994. He received the B.Sc. degree from Nanchang Hangkong University, in 2018, where he is currently pursuing the M.E. degree. His research interests include ultrasound TOFD detection imaging algorithms and image processing.

YUAN TANG was born in Chongqing, China, in 1996. He received the B.E. degree from Chongqing University of Posts and Telecommunications, in 2020, where he is currently pursuing the M.E. degree. His research interests include ultrasonic testing technology and circuit design.

ZHIHENG CHEN was born in Jiangxi, China, in 1997. He received the B.Sc. degree from Nanchang Hangkong University, in 2018, where he is currently pursuing the M.E. degree. His research interests include ultrasound imaging algorithms and image processing.